Pattern Recognition by Electrical Coupling of Eight Chemical Reactors

W. Hohmann, M. Kraus, and F. W. Schneider*

Institute of Physical Chemistry, University of Wuerzburg, Am Hubland, 97074 Wuerzburg, Germany

Received: May 5, 1999; In Final Form: July 20, 1999

On the basis of our experiments and simulations on pattern recognition and learning, we have extended the previous four reactor network to eight reactors which are electrically coupled via Pt-working electrodes in the fashion of a Hopfield network. This extension considerably improves the recognition processes and allows to encode three reactor patterns. Since each of the eight reactors can be either in a periodic (P) or a nodal (N) steady state using the Belousov−Zhabotinsky (BZ) reaction, there are 256 ($=2^8$) dynamical patterns of which any three patterns may be encoded in the reactor net. We describe the recognition processes that successfully associate some of the remaining 253 patterns (including mirror images) as initial patterns to one of the encoded patterns to which it has the least number of errors. The advantages and limitations of electrical coupling versus mass coupling are discussed. Numerical simulations using the seven-variable Montanator by Györgyi and Field are in agreement with the experiments.

Introduction

In previous work[1−3] on pattern recognition we have used reactor networks that consisted of four chemical reactors that were electrically coupled by Pt-working electrodes in the fashion of a Hopfield network. The recognition processes were carried out by the Belousov−Zhabotinsky (BZ) reaction in either a focal[1] or oscillatory[2,3] free-running state. The reactor networks were capable of associating presented phase patterns (in-phase or out-of-phase[1,2]) with stored patterns using local and global coupling. In our first study,[1] recognition was achieved by starting with focal steady states in the BZ reaction. The focal steady states were perturbed by sinusoidal oscillations of the electric potential resulting in a homogeneous initial pattern (all four reactors oscillating in-phase). This external sinusoidal perturbation corresponded to a global coupling of all four reactors. The recognition process was initiated by activating local coupling which consisted of time delayed feedback interactions. As a result, a recall of one of the two stored phase patterns was achieved with a 50% probability in many experiments. In our second study,[2] we started with all four reactors in their oscillatory region. We employed entraining pulses of electrical current as global coupling of all four reactors which lead to a 1:2 response of the oscillatory period. Thus, all possible phase patterns (in-phase and out-of-phase) could be used as initial patterns and a unique recognition of either of two encoded patterns was possible.

In a third study on learning and recognition,[3] we excluded global coupling altogether and employed only local coupling of four reactors according to Hopfield.[4] Instead of using different phase patterns (in-phase or out-of-phase), we placed each reactor in one of two dynamical states: a periodic (P state) or a nodal excitable steady (N state) in analogy to a firing or a silent in-vivo neuron. The transition between the two states is described by a saddle node infinite period (SNIPER) bifurcation[2] with the electric current as a bifurcation parameter. Thus the value of the electric current determines whether a given reactor is in a P (zero or low current) or in a N (high current) state. The process of recognition involves transitions between the two reactor states P and N, where a set of states represents a pattern. In order to successfully associate any presented initial pattern with an encoded pattern, it becomes necessary to introduce an averaging procedure of the response potential. As a result, a successful recognition process rapidly associates a presented pattern with the encoded pattern to which it has the least number of errors.

The present report describes an extension of our previous four-reactor networks[1−3] to a larger reactor network consisting of eight electrically coupled reactors. The larger network has new qualities: more than two dynamical patterns may be encoded, each reactor is actively coupled to every other reactor as in a general Hopfield net,[4] and individual coupling strengths may be unequal.

A Hopfield net is characterized by a coupling matrix whose entries are the coupling strengths between the individual reactors. This coupling matrix is calculated for all encoded patterns by a Hebbian type rule.[5] Its entries may be either positive ($w_{ij} > 0$) or negative ($w_{ij} < 0$) depending on whether a coupling interaction is attractive or repulsive, respectively. An attractive interaction will drive two coupled reactors into identical (PP or NN) dynamic states whereas a repulsive interaction will favor mixed (PN) states. We achieve both attractive and repulsive coupling by using the time-averaged electric potential of a reactor as the weighted input to another reactor. This procedure allows kinetic transitions from either N to P or P to N. However, any phase information is thereby lost.

Laplante et al. (LPHR)[6] were the first to experimentally perform pattern recognition by using mass coupling via reciprocal pumping in a network of eight chemical reactors and 24 connections which contained the bistable (nonoscillatory) iodate−arseneous acid reaction. Since mass coupling is restricted to positive coupling, the number of patterns to be successfully associated is limited.

Experimental Section

Eight CSTRs (continuous flow stirred tank reactors) of 4.2 mL volume each are electrically coupled via Pt-working

* To whom correspondence should be addressed.

10.1021/jp991480n CCC: $18.00
Published on Web 08/31/1999

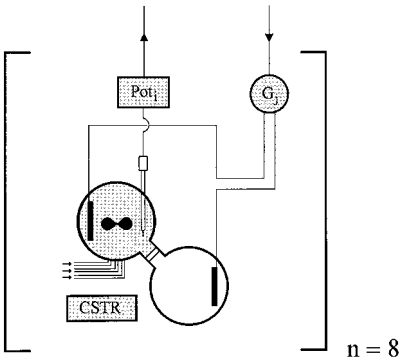

Figure 1. Each of the eight coupled CSTRs ($n = 8$) has its own reference reactor with a Teflon membrane. The redox potentials Pot_i are monitored by Pt/Ag/AgCl redox electrodes at 1 Hz. The individual Pot_i are averaged by a PC and used in eq 3 to calculate the currents $G_j(t)$, which are applied via galvanostats to the Pt-working electrodes in each reactor.

electrodes (~2.0 cm^2).[3] Each reactor also contains a Pt/Ag/AgCl redox electrode and a magnetic stirrer (600 rpm). A Teflon membrane connects each reactor with its half-cell. The latter also contains a Pt-working electrode and sulfuric acid (0.4 mol/L). Three reactant streams feed three reactant solutions into each reactor by three precise piston pumps at identical flow rates with three syringes (50 mL each). Syringe I delivers $NaBrO_3$ (0.42 mol/L); syringe II $Ce_2(SO_4)_3$ (1.5×10^{-3} mol/L) and malonic acid (0.9 mol/L); and syringe III sulfuric acid (1.125 mol/L). The flow rate is fixed at $k_f = 6.0 \times 10^{-4}$ s^{-1} with a residence time of 27.8 min in order to establish free running P1 oscillations ($T = 33$ s). The redox potentials Pot_i in each reactor are measured and digitally monitored at 1 Hz. The redox potentials are normalized due to variations in the sensitivities of the redox electrodes and presented in arbitrary units. Each Pt-working electrode receives its current from a separate galvanostat (G_i, E&G Instruments). All currents are reevaluated every second. The averaged output $Pot_{i,av}$ of a Pt/Ag/AgCl redox electrode determines the input $G_j(t)$ to the Pt-working electrodes of the neighboring reactor(s) according to eq 3.

SNIPER Bifurcation. Recently we discovered[2] that the application of an electric current to the free-running oscillatory BZ reaction causes a transition from the oscillatory to a nodal steady state. Close to the transition point the oscillation frequency gradually declines to zero whereas the amplitude remains constant up to the bifurcation point where it abruptly disappears. This so-called SNIPER (saddle node infinite period) bifurcation occurs at a current of 0.85 mA for $k_f = 6.0 \times 10^{-4}$ s^{-1}, where a limit cycle "collides" with a saddle node leading to an "oscillation of infinite period".[7−13] In our experiments we use the SNIPER scenario to switch between the oscillatory (P) and nodal (N) states where the initial P state is set at a current of 0.45 mA (period $T = 35$ s) and the N state at 1.15 mA (Figure 2). The nodal steady state has been assigned 1000 arb units.

Hopfield Network. A Hopfield network is analogous to a spin-glass model and the coupling strengths between individual units are summarized in matrix notation.[4] Thus the Hopfield matrix is a 8×8 matrix for the present reactor network. In order to establish the Hopfield matrix for the encoded patterns the following Hebbian-type rule[5] is used:

If two reactors of an encoded pattern are in the same state, (i.e., P−P or N−N) the coupling strength is +1 (attractive interaction), whereas if the two states are unlike (i.e., P−N or N−P), it is −1 (repulsive interaction). For all encoded patterns the individual coupling strengths are added and the sum is entered into the Hopfield matrix. This is expressed in bipolar

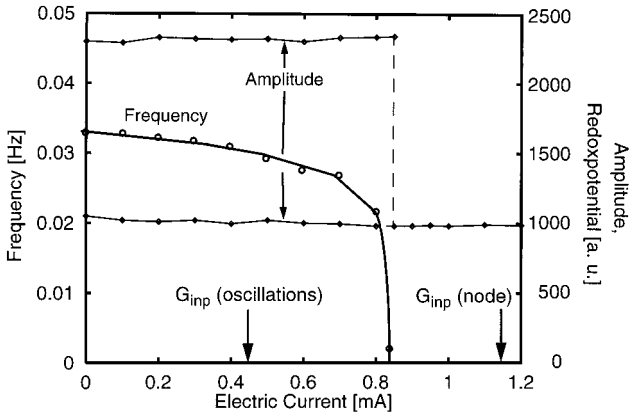

Figure 2. Experimental SNIPER bifurcation at 0.85 mA with the electrical current (mA) as a bifurcation parameter at $k_f = 6.0 \times 10^{-4}$ s^{-1}. The frequency of the oscillations (P state) decreases to zero whereas the amplitudes remain almost constant and disappear suddenly at the SNIPER point. The redox potential of the nodal steady state N is almost constant at 1000 arbitrary units. G_{inp} is a bias current in eq 3 in order to establish either oscillations (0.45 mA) or a node (1.15 mA).

TABLE 1

	patterns to be encoded and their mirror patterns					
CSTR	1	2	3	M1	M2	M3
1	P	N	P	N	P	N
2	N	P	P	P	N	N
3	P	P	N	N	N	P
4	P	N	N	N	P	P
5	N	N	P	P	P	N
6	N	P	N	P	N	P
7	N	P	P	P	N	N
8	P	N	N	N	P	P

notation[14] as

$$w_{ij} = \sum_{1}^{p} x_i^s x_j^s \qquad \text{for } i \neq j$$
$$w_{ij} = 0 \qquad \text{for } i = j \tag{1}$$

where w_{ij} is the coupling strength between reactor i and j, x_i^s is the bipolar notation of the dynamic state in reactor i of pattern s, and p is the number of patterns (=3) to be encoded. Since the matrix is symmetrical the mirror images of the dynamic patterns are encoded as well.

Encoding Three Patterns in Eight Reactors. A reactor network consisting of eight reactors can be encoded by maximally three patterns. Empirically, for a very large reactor network the number of patterns to be encoded[14] is $p \approx 0.25N$, where N is the total number of reactors. As an example, we show the Hopfield matrix for the same three patterns (in bipolar notation) (Table 1) as those of LPHR, in order to facilitate a comparison between electrical and active mass coupling.

Thus, for patterns 1, 2, and 3 (Table 1) the following Hopfield matrix is obtained as

$$W = \begin{pmatrix} 0 & -1 & -1 & +1 & +1 & -3 & -1 & +1 \\ -1 & 0 & -1 & -3 & +1 & +1 & +3 & -3 \\ -1 & -1 & 0 & +1 & -3 & +1 & -1 & +1 \\ +1 & -3 & +1 & 0 & -1 & -1 & -3 & +3 \\ +1 & +1 & -3 & -1 & 0 & -1 & +1 & -1 \\ -3 & +1 & +1 & -1 & -1 & 0 & +1 & -1 \\ -1 & +3 & -1 & -3 & +1 & +1 & 0 & -3 \\ +1 & -3 & +1 & +3 & -1 & -1 & -3 & 0 \end{pmatrix} \tag{2}$$

as W contains positive as well as negative entries (±1 and ±3): Since a given reactor does not couple onto itself (eq 1), the diagonal is zero.

One may display the general scheme, where each of the 28 connections is bidirectional, as

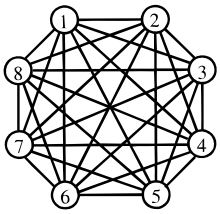

Note that for active mass coupling only the positive entries can be realized experimentally (12 bidirectional connections as used by LPHR). For electrical coupling the electrical currents $G_j(t)$ are applied to the individual reactors j via the Pt-working electrodes (eq 3) and $G_{\mathrm{inp}i}$(bias) is set equal to 0.45 mA (1.15 mA) for an initial periodic (nodal) state. $\mathrm{Pot}_{i,\mathrm{av}}(t)$ is the averaged redox potential over the previous 100 s which is recalculated every second, and w_{ij} are the coupling strengths between reactors i and j. The averaging procedure has been carried out in order to avoid periodic crossings of the threshold when a transition from a P to a N state is necessary for recognition.

We write the expression for the electrical currents $G_j(t)$ in matrix form:

$$\begin{pmatrix} G_{\mathrm{inp1}} & -1 & -1 & +1 & +1 & -3 & -1 & +1 \\ -1 & G_{\mathrm{inp2}} & -1 & -3 & +1 & +1 & +3 & -3 \\ -1 & -1 & G_{\mathrm{inp3}} & +1 & -3 & +1 & -1 & +1 \\ +1 & -3 & +1 & G_{\mathrm{inp4}} & -1 & -1 & -3 & +3 \\ +1 & +1 & -3 & -1 & G_{\mathrm{inp5}} & -1 & +1 & -1 \\ -3 & +1 & +1 & -1 & -1 & G_{\mathrm{inp6}} & +1 & -1 \\ -1 & +3 & -1 & -3 & +1 & +1 & G_{\mathrm{inp7}} & -3 \\ +1 & -3 & +1 & +3 & -1 & -1 & -3 & G_{\mathrm{inp8}} \end{pmatrix} \cdot \begin{pmatrix} w_{1j} & \mathrm{Pot}_1 \\ w_{2j} & \mathrm{Pot}_2 \\ w_{3j} & \mathrm{Pot}_3 \\ w_{4j} & \mathrm{Pot}_4 \\ w_{5j} & \mathrm{Pot}_5 \\ w_{6j} & \mathrm{Pot}_6 \\ w_{7j} & \mathrm{Pot}_7 \\ w_{8j} & \mathrm{Pot}_8 \end{pmatrix} = \begin{pmatrix} G_1(t) \\ G_2(t) \\ G_3(t) \\ G_4(t) \\ G_5(t) \\ G_6(t) \\ G_7(t) \\ G_8(t) \end{pmatrix} \quad (3)$$

where $\mathrm{Pot}_i = \mathrm{Pot}_{i,\mathrm{av}}(t) - 1000$ and $w_{jj}\mathrm{Pot}_j = 1$, j being the reactor number.

As an example, for $j = 1$

$$G_1(t) = G_{\mathrm{inp1}} - w_{21}\mathrm{Pot}_2 - w_{31}\mathrm{Pot}_3 + w_{41}\mathrm{Pot}_4 + w_{51}\mathrm{Pot}_5 - 3w_{61}\mathrm{Pot}_6 - w_{71}\mathrm{Pot}_7 + w_{81}\mathrm{Pot}_8$$

Since the nodal steady state is chosen as the reference state, we subtract 1000 arbitrary units from $\mathrm{Pot}_{i,\mathrm{av}}$, i.e., there is no contribution $w_{ij}(\mathrm{Pot}_{i,\mathrm{av}} - 1000)$ of reactor i to $G_j(t)$ if it is in a nodal steady state. On the other hand, any potential between 1000 and ~1400 au (the maximal $\mathrm{Pot}_{i,\mathrm{av}}(t)$) may be used as a reference state.

Results and Discussion

The number of ways to combine 256 ($=2^8$) dynamical patterns in groups of three patterns is $\sim 2.76 \times 10^6$ ($=256!/253!3!$). For a complete documentation this would require $\sim 354 \times 10^6$ ($=2.76 \times 10^6(256/2)$) recognition experiments where the number of patterns is 256; the factor of $^1/_2$ is introduced in order not to count equivalent mirror patterns. This astronomical number cannot be realized experimentally, of course. We have done recognition experiments with several sets of three encoded patterns with about 30 different initial patterns. As representative examples we report only the recognition experiments of encoded patterns 1, 2, and 3 with initial patterns A, B, C, and D (Figures 3−6). We found it experimentally convenient to adjust the coupling strengths in such a way that a successful transition from P to N occurs only when the net-coupling strength ($\sum w_{ij}$) into reactor j is -4 or more negative. Conversely, a N to P transition occurs only if the net-coupling strength is $+3$ or larger in our experiments. Due to our definition of the reference state a positive current stands for a negative w_{ij} and vice versa.

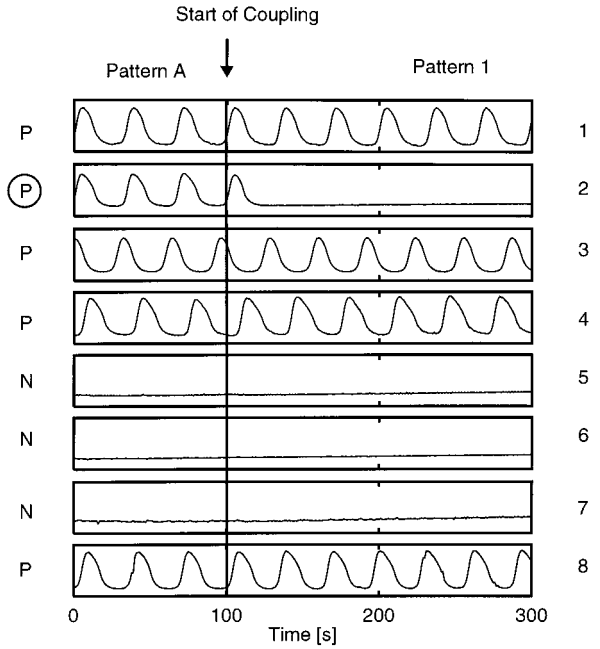

Figure 3. Experimental time series of all eight electrically coupled reactors for the recognition of pattern A. Pattern A is associated with encoded pattern (1 error) immediately after the start of electrical coupling at 100 s. The error P (circled) in reactor 2 is corrected to N.

Pattern A (Initial Pattern). In order to demonstrate a one-error recognition process we have chosen the initial pattern A which shows 1 error relative to encoded pattern 1, and 5 errors relative to encoded patterns 2 and 3. One has to keep in mind that only P states make any contributions to the $G_j(t)$ currents in the present experiments, since we have selected a nodal N state as the reference state. Therefore, only reactors 1, 3, 4, and 8 contribute to $G_2(t)$. In other words, the net coupling strength $\sum w_{i2}$ is equal to -8, since $w_{12} = -1$, $w_{32} = -1$, $w_{42} = -3$, and $w_{82} = -3$ all show negative entries. Thus, a strong positive current $G_2(t)$ is delivered into reactor 2, driving it into a N state (Figure 2). All other reactor states remain unchanged as seen from the W-matrix (eq 2). As a result, the recognition experiment (Figure 3) rapidly associates pattern A with pattern 1 involving a transition from a P to a N state in reactor 2 within one oscillation (i.e., ~20 s).

Pattern B (Initial Pattern). The initial pattern B was chosen as an example to show how 2 errors relative to encoded pattern 3 and relative to the mirror image M1 of pattern 1 are successfully corrected (Figure 4). A recall of pattern 3 would involve a transition of reactor 2 from N to P as well as reactor 6 from P to N. Surprisingly, rather than pattern 3 it is M1 which

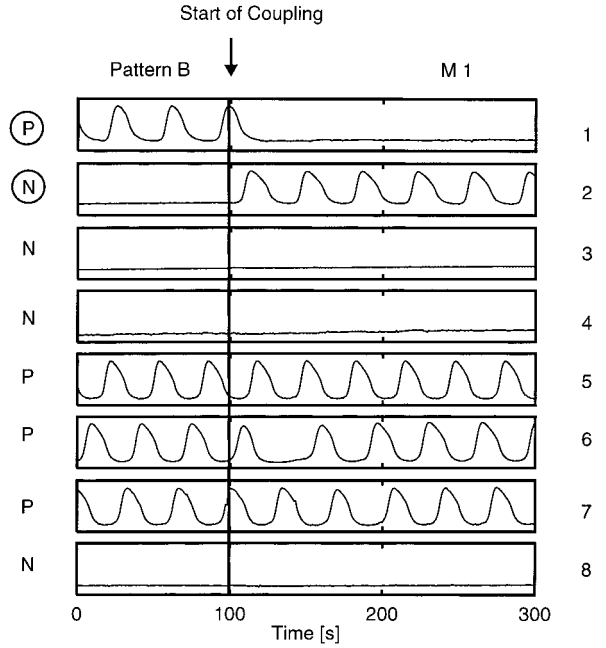

Figure 4. Experimental time series of all eight reactors for the recognition of pattern B which shows 2 errors (P and N in reactors 1 and 2, respectively) with respect to the mirror pattern M1. Both errors are corrected; for details see text.

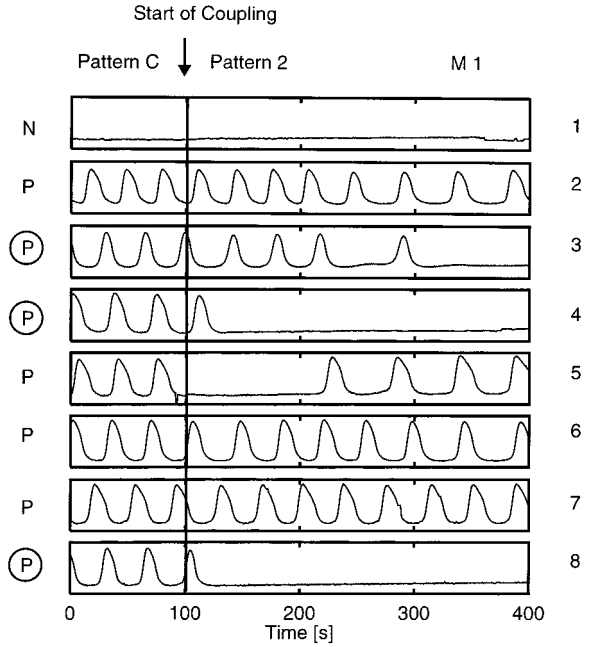

Figure 5. Experimental time series of all eight reactors for the recognition of pattern C which shows 3 errors with respect of pattern 2 and M1. After the start of electrical coupling, pattern C is transiently associated with pattern 2 and settles rapidly into pattern M1. Thus 3 errors (in reactors 3, 4, and 8) relative to M1 have been corrected.

is always selected involving a transition from P to N of reactor 1 and N to P of reactor 2. The reason for the preference of pattern M1 is the complex dynamics of the coupling process: The current into reactor 2 ($G_2(t)$) is decreased, since only the P states of reactors 1, 5, 6, and 7 make any coupling contributions to $G_2(t)$ causing a net increase in $\sum w_{i2}$ of $+4$ ($w_{12} = -1$, $w_{52} = +1$, $w_{62} = +1$, $w_{72} = +3$). This converts reactor 2 from N to P. As a consequence, contributions of reactor 2 to reactors 1 and 6 become decisive: Since reactor 2 is now in a P state, a positive current into reactor 1 ($w_{21} = -1$) is created over and above the already existing contributions of reactors 5, 6, and 7 which, by themselves, are not able to cause a transition of reactor 1 from P or N since $\sum w_{i1} = -3$. Conversely, reactor 6 receives momentarily a net positive current ($\sum w_{i6} = -3$) due to the contributions of the oscillating reactor 1 ($w_{56} = -3$), reactor 5 ($w_{15} = -1$) and reactor 7 ($w_{76} = +1$) resulting in a transiently prolonged period (Figure 4) immediately after the start of coupling. Due to the change in dynamics of reactors 1 and 2 the net-contribution to reactor 6 is a negative current ($\sum w_{i6} = +1$) ($w_{26} = +1$, $w_{56} = -1$, and $w_{76} = +1$). Therefore, reactor 6 remains in the P state. Thus pattern M1 is recalled and not pattern 3. The rate of recognition is very high, i.e., practically instantaneously for reactors 1 and 2, whereas reactor 6 takes about 40 s to remain in the P state.

Pattern C (Initial Pattern). The initial pattern C shows 3 errors relative to the following patterns: pattern 2, pattern M1, and pattern M3. The recognition process corrects all errors. It involves a transient recall of pattern 2 after which the network settles into pattern M1 (Figure 5). This behavior is more complex than that of pattern B due to several changes of states causing corresponding changes in the currents.

Pattern D (Initial Pattern). As a consequence of our choice of the nodal state as the reference, a pattern containing more than five N states becomes dynamically "inert", since their contributions to $G_j(t)$ are zero. As one of the few examples of a failure to complete recognition we present pattern D which contains 6 N states and 2 errors relative to patterns 2 as well as M1 (Figure 6). Interestingly, the recognition process does correct

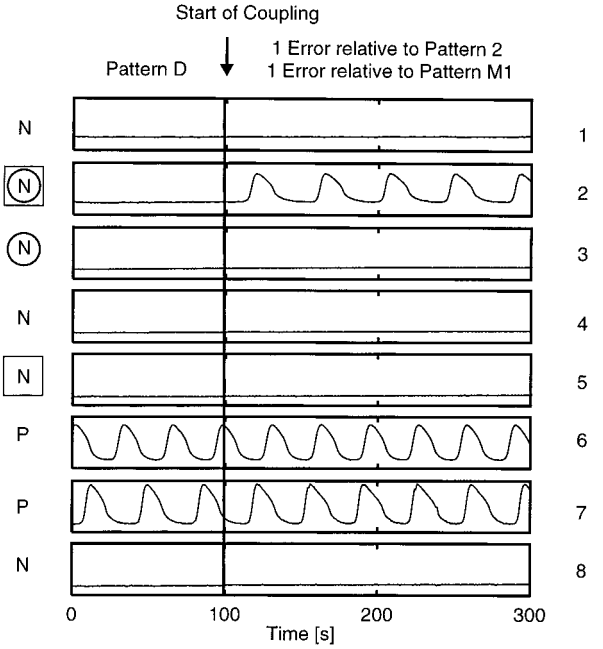

Figure 6. Experimental time series of all eight reactors for the recognition of pattern D wich consists of 6 N states and shows 2 errors relative to pattern 2 (circles) and 2 errors to pattern M1 (squares). Only the common error in reactor 2 has been corrected whereas reactor 3 and reactor 5 have not changed due to the high number (>5) of N states in the inital pattern; see text.

reactor 2 (from N to P) which represents a common error in both patterns 2 and M1. The reason is the strong net-coupling strength ($w_{62} = +1$ and $w_{72} = +3$) of $+4$ which corresponds to a strong decrease of $G_2(t)$ after coupling has taken place. However, the second error (either reactor 3 in pattern 2 or reactor 5 in pattern M1) has not been corrected by the network, since the net-coupling strength $\sum w_{i3}$ for reactor 3 is -1 and for reactor 5 is $+1$ only. Both net coupling strengths are insufficient to cause a transition from N to P with the present reference state.

Other Patterns. As an example of the versatility of electrical coupling, pattern (PPNPPPPP) was offered as an initial pattern showing 3 errors with respect to patterns 3, M1, and M2 and, in addition, 5 errors with respect to patterns 1, 2 and M3. Pattern 3 was uniquely selected in several identical experiments (not shown). This is in contrast to mass coupling where pattern 3 could not be selected except if it was presented as an initial pattern.

As another example, pattern 2 was always selected from initial patterns (NPPPNPPN, NPPNNPPP, and NPPNNNPN) which showed one error with respect to pattern 2 and more than one error to the other encoded patterns. This is also in contrast to the observations of LPHR who reported the selection of pattern 1 most of the time, even when the initial conditions were chosen to be closer to pattern 2 or 3.

Comparison with Mass Coupling

For mass coupling the Hopfield matrix W is constructed identically as for the present electrical coupling except that negative entries are set equal to zero. Thus, only positive terms and zeros are contained in W for mass coupling, which limits the number of patterns to be recognized. In contrast, any encoded pattern (or its mirror image) can be recognized from an error-prone pattern in electric coupling if it contains no more than 5 N states here. Since a SNIPER bifurcation is relatively sharp, the recognition process is more efficient than in a bistable reaction where the dynamics depends strongly on initial conditions, i.e., on the position of the system relative to the equistability point in the bistability region (6).

In work with mass coupling, LPHR displayed three recognition experiments (their Figures 1−3) for encoded patterns 1−3 where the bistable steady states correspond to the present P and N states. For an initial pattern corresponding to the mirror image of pattern B, the recognition process corrected two errors (reactors 1 and 2) to obtain pattern 1 (or its mirror image). This is in essential agreement with the recognition process for the present pattern B (Figure 4) which leads to pattern M1. With mass coupling LPHR obtained a transient homogeneous pattern and, in another experiment, a final homogeneous pattern after a mirror image of a stored pattern was transiently observed at a reactant flow rate lower than the equistability point within the bistability region. With electric coupling such homogeneous patterns are not observed except if the initial pattern is a homogeneous N state pattern. Whereas pattern 3 could also be recognized in electrical coupling, this was apparently not possible in mass coupling unless pattern 3 itself was presented as an initial pattern.

Both coupling methods are quite robust within their regions of applicability. Electrical coupling via Pt-working electrodes is very rapid taking seconds instead of minutes and hours since a nonlinear chemical reaction is very sensitive toward extremely small changes in concentrations of intermediates at the Pt electrode. Both methods do show restrictions (only positive coupling strengths for mass coupling and not more than 5 N states in a pattern for the presently chosen reference state (1000 au) in electrical coupling). Although electrical coupling is more practical and versatile, it has the disadvantage of having to use a computing device to calculate the currents $G_j(t)$ to be delivered to the individual reactors. Furthermore, the averaging procedure for the realization of negative coupling removes any phase information in the oscillatory responses.

Numerical Simulations

Our numerical simulations of the experiments are based on the seven-variable Montanator by Györgyi and Field.[1−3,15] The mechanism contains two cycles describing the autocatalytic production of $HBrO_2$ and the formation of Br^- (Table 2) with rate constants and concentrations given in Table 3. The seven variables are bromous acid, bromide, bromate, bromomalonic acid and its radical, Ce^{3+}, and Ce^{4+}. We include the effect of the electric current by adding the term $C[Ce^{4+}]$ to the rate equation for $[Ce^{3+}]$ and subtracting the term $C[C^{4+}]$ from the rate equation of $[Ce^{4+}]$:

$$d[Ce^{3+}]/dt = f([Ce^{3+}]) - k_f([Ce^{3+}] - [Ce^{3+}]_0) + C[Ce^{4+}]$$

$$d[Ce^{4+}]/dt = f([Ce^{4+}]) - k_f([Ce^{4+}] - C[Ce^{4+}]) \quad (4)$$

where C is proportional to the amount of charge deposited at the Pt-working electrode. $[Ce^{3+}]_0$ is the inflow concentration and $f([Ce^{3+}])$ describes the rate equations of the model. As a result, for $k_f = 3.0.5 \times 10^{-4}$ s^{-1}, P1 oscillations are obtained from $C = 0$ to $C = 0.11$. At $C = 0.11$ a SNIPER bifurcation occurs in agreement with the experiments. For $C > 0.11$ a nodal steady state exists.[2] For all C values an instable focus also exists as calculated by the continuation method (not shown).

Recognition of Patterns. For a direct comparison with the experiment we show the simulated recognition process for pattern A (Figure 7) which has one error relative to pattern 1. It is immediately seen that the recognition process takes several oscillation periods in contrast to the experimental case. The model shows a greater sensitivity toward perturbations than the experimental system. Therefore, the averaging procedure has to be carried out over more oscillations than in the experiment. The individual currents have also been simulated (Figure 7). Only the C value of reactor 2 crosses threshold leading to the desired transition from a P to a N state. It is noteworthy that the level ($[Ce^{4+}]$) of the nodal steady state is substantially higher than the averaged $[Ce^{4+}]_{ave}$ of a P state in contrast to the experiments where the $[Ce^{4+}]_{ave}$ of the nodal steady state is always equal to or lower than that of the averaged oscillatory state. In all cases the simulations were in essential agreement with the experiments.

TABLE 2: Seven-Variable Montanator (Nonstoichiometric Steps)[a]

$HBrO_2 + Br^- + H^+$	→	2BrMA	(1)
$BrO_3^- + Br^- + 2\,H^+$	→	$HBrO_2$ + BrMA	(2)
$2HBrO_2$	→	$BrO_3^- + BrMA + H^+$	(3)
$BrO_3^- + HBrO_2 + H^+$	→	$2BrO_2^\bullet + H_2O$	(4)
$2BrO_2^\bullet + H_2O$	→	$BrO_3^- + HBrO_2 + H^+$	(5)
$Ce^{3+} + BrO_2^\bullet + H^+$	→	$HBrO_2 + Ce^{4+}$	(6)
$HBrO_2 + Ce^{4+}$	→	$Ce^{3+} + BrO_2^\bullet + H^+$	(7)
$MA + Ce^{4+}$	→	$MA^\bullet + Ce^{3+} + H^+$	(8)
$BrMA + Ce^{4+}$	→	$Ce^{3+} + Br^-$	(9)
$MA^\bullet$ + BrMA	→	$MA + Br^-$	(10)
$2MA^\bullet$	→	MA	(11)

[a] MA = malonic acid; $MA^\bullet$ = malonic acid radical; BrMA = bromomalonic acid.

TABLE 3: Rate Constants and Concentrations of Seven-Variable Montanator

$k_1 = 2.0 \times 10^6$ s^{-1} M^{-2}	$k_2 = 2.0$ s^{-1} M^{-3}
$k_3 = 2.0 \times 10^3$ s^{-1} M^{-1}	$k_4 = 3.3 \times 10^1$ s^{-1} M^{-2}
$k_5 = 7.6 \times 10^5$ s^{-1} M^{-2}	$k_6 = 6.2 \times 10^4$ s^{-1} M^{-2}
$k_7 = 7.0 \times 10^3$ s^{-1} M^{-1}	$k_8 = 3.0 \times 10^{-1}$ s^{-1} M^{-1}
$k_9 = 3.0 \times 10^{-1}$ s^{-1} M^{-1}	$k_{10} = 2.4 \times 10^4$ s^{-1} M^{-1}
$k_{11} = 3.0 \times 10^9$ s^{-1} M^{-1}	
$[MA]_0 = 0.25$ M	$[H^+]_0 = 0.26$ M
$[Ce^{3+}]_0 = 8.33 \times 10^{-4}$ M	$[BrO_3^-]_0 = 0.1$ M
$[H_2O] = 55$ M	

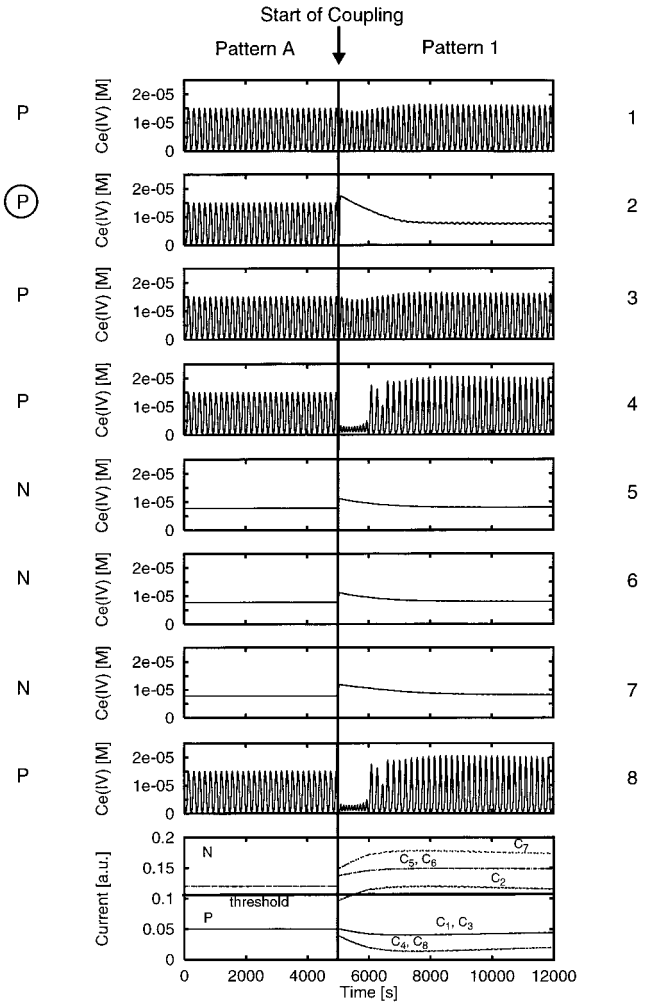

Figure 7. Computer simulations of the time series of all eight reactors and their currents (C_1-C_8, bottom) for the recognition of pattern A. In agreement with the experiment (Figure 3), pattern A is associated with pattern 1 (1 error in reactor 2) after several oscillation periods. Notice the expanded time scale with respect to the experiment. Only C_2 crosses threshold while all other currents remain above (N state: C_5, C_6, and C_7) or below (P state: C_1, C_2, C_4, and C_8).

Conclusions

In the present 8-reactor network, an initial pattern containing errors is always associated with the particular encoded pattern (or its mirror image) to which it has the least number of errors. If there are several encoded patterns to which it has the same number of errors then a particular pattern is always selected, although another encoded equal-error pattern may appear transiently. The recognition process is very robust and reliable,

If an encoded pattern is offered as an initial pattern it is immediately recalled,

If an initial pattern contains more than five N (nodal) states, complete recognition is not possible for the present choice of the nodal reference state (1000 arb units at 1.15 mA) which does not contribute to any coupling interaction. However, by a judicious choice of the reference state (between 1400 and 1000 arb units) this restriction may be lifted at the expense of a higher experimental sensitivity,

In order to encode four (instead of three) patterns a larger reactor network consisting of ∼16 reactors is necessary,

Electrical coupling has been reliably simulated on the computer in this work on the basis of an appropriate rate model. Therefore, the experimental implementation of very large reactor networks[18−20] may become a tour de force in combining the complexities of nonlinear chemistry with technical methods such as microtechniques.

Acknowledgment. We thank N. Schinor for technical assistance and the Deutsche Forschungsgemeinschaft and the Fonds der Chemischen Industrie for financial support.

References and Notes

(1) Dechert, G.; Zeyer, K.-P.; Lebender, D.; Schneider, F. W. *J. Phys. Chem.* **1996**, *100*, 19043.

(2) Hohmann, W.; Kraus, M.; Schneider, F. W. *J. Phys. Chem.* **1997**, *101*, 7364.

(3) Hohmann, W.; Kraus, M.; Schneider, F. W. *J. Phys. Chem.* **1998**, *102*, 3111.

(4) Hopfield, J. J. *Proc. Natl. Acad. Sci. U.S.A.* **1982**, *79*, 2554; **1984**, *81*, 3088.

(5) Hebb, D. O. In *Neurocomputing: Foundations of Research*; Anderson, J. A., Rosenfeld E., Eds.; MIT Press: Cambridge, MA, 1988.

(6) Laplante, J.-P.; Pemberton, M.; Hjelmfelt, A.; Ross, J. *J. Phys. Chem.* **1995**, *99*, 10063.

(7) Andronov, A. A.; Witt, A. A.; Khaikin, S. E. In *Theory of Oscillators*; Pergamon: Oxford, UK, 1966.

(8) Boissonade, J.; De Kepper, P. *J. Phys. Chem.* **1980**, *84*, 501.

(9) De Kepper, P.; Boissonade, J. *J. Chem. Phys.* **1981**, *75*, 189.

(10) Maselko, J.; Epstein, I. R. *J. Phys. Chem.* **1984**, *88*, 5305.

(11) Noszticzius, Z.; Stirling, P.; Wittmann, M. *J. Phys. Chem.* **1985**, *89*, 4914.

(12) Gaspar, V.; Galambosi, P. *J. Phys. Chem.* **1986**, *90*, 2222.

(13) Noszticzius, Z.; Wittmann, M.; Stirling, P. *J. Chem. Phys.* **1987**, *86*, 1922.

(14) Zupan, J.; Gasteiger, J. *Neural Networks for Chemists*; VCH Verlag: Weinheim, Germany, 1993

(15) Györgyi, L.; Field, R. J. *J. Phys. Chem.* **1991**, *95*, 6594; *Nature* **1992**, *355*, 808.

(16) Gear, C. W. *Numerical Initial Value Problems in Ordinary Differential Equations*; Prentice Hall: Englewood Cliffs, NJ, 1971.

(17) Shampine, L. F.; Gear, C. W. *SIAM Rev.* **1979**, *21*, 1.

(18) Hjelmfelt, A.; Ross, J. *Proc. Natl. Acad. Sci. U.S.A.* **1994**, *91*, 63.

(19) Hjelmfelt, A.; Schneider, F. W.; Ross, J. *Science* **1993**, *260*, 335.

(20) Hjelmfelt, A.; Ross, J. *J. Phys. Chem.* **1993**, *97*, 7988.